

# muon $g - 2$ anomaly and $\mu$ - $\tau$ -philic Higgs doublet with a light CP-even component

Hong-Xin Wang<sup>1</sup>, Lei Wang<sup>1</sup>, Yang Zhang<sup>2</sup>

<sup>1</sup> *Department of Physics, Yantai University, Yantai 264005, P. R. China*

<sup>2</sup> *School of Physics and Microelectronics,  
Zhengzhou University, Zhengzhou 450001, P. R. China*

## Abstract

We examine the possibilities of accommodating the muon  $g - 2$  anomaly reported by Fermilab in the 2HDM with a discrete  $Z_4$  symmetry in which an inert Higgs doublet field ( $H$ ,  $A$ ,  $H^\pm$ ) has the lepton flavor violation  $\mu$ - $\tau$  interactions. We study the case of light  $H$  ( $5 \text{ GeV} < m_H < 115 \text{ GeV}$ ) and assume the Yukawa matrices to be real and symmetrical. Considering relevant theoretical and experimental constraints, especially for the multi-lepton searches at the LHC, we find the muon  $g - 2$  anomaly can be explained within  $2\sigma$  range in the region of  $5 \text{ GeV} < m_H < 20 \text{ GeV}$ ,  $130 \text{ GeV} < m_A$  ( $m_{H^\pm}$ )  $< 610 \text{ GeV}$ , and  $0.005 < \rho < 0.014$ . Meanwhile, the  $\chi_\tau^2$  fitting the data of lepton flavour universality in the  $\tau$  decays approaches to the SM prediction.

## I. INTRODUCTION

The Fermilab collobartion presented the new result for muon anomalous magnetic moment  $g - 2$  which now, combined with the data of the E821 [1], amounts to [2]

$$\Delta a_\mu = a_\mu^{exp} - a_\mu^{SM} = (251 \pm 59) \times 10^{-11}. \quad (1)$$

The experimental value has an approximate  $4.2\sigma$  discrepancy from the SM prediction.

Two-Higgs-doublet model (2HDM) is a simple extension of SM by adding another Higgs doublet field. The muon  $g - 2$  anomaly can be simply explained in the lepton-specific 2HDM [3–15] and aligned 2HDM [16–25]. However, the tree-level diagram mediated by the charged Higgs gives negative contribution to the decay  $\tau \rightarrow \mu\nu\bar{\nu}$ , which will raise the deviation of the LFU in  $\tau$  decays [12–14]. Besides, a scalar with the  $\mu$ - $\tau$  LFV interactions can accommodate the muon  $g - 2$  anomaly by the contribution of one-loop diagrams [26–38]. Meanwhile, the extra Higgs doublet with the  $\mu$ - $\tau$  LFV interactions can alleviate the discrepancy of LFU in  $\tau$  decays [33]. In this paper, we consider relevant theoretical and experimental constraints, including the LUF in the  $\tau$  decays and multi-lepton event searches at the LHC, and examine the possibilities of explaining the muon  $g - 2$  anomaly reported by Fermilab in the 2HDM with a discrete  $Z_4$  symmetry in which an inert Higgs doublet field ( $H$ ,  $A$ ,  $H^\pm$ ) has the lepton flavor violation  $\mu$ - $\tau$  interactions. Ref. [35] applied the model to discuss the E821 result of muon  $g - 2$  anomaly combining the LUF in the  $\tau$  decays and multi-lepton event searches at the LHC, and examined the case of  $m_H > 200$  GeV. Different from the Ref. [35], we study the case of light  $H$  ( $5 \text{ GeV} < m_H < 115 \text{ GeV}$ ) in the paper.

Our work is organized as follows. In Sec. II we introduce the model briefly. In Sec. III we discuss the muon  $g - 2$ , the LUF in  $\tau$  decays, the exclusion limits of multi-lepton event searches at the LHC, and other relevant constraints. In Sec. IV, we show the allowed and excluded paramter space. Finally, we give our conclusion in Sec. V.

## II. THE 2HDM WITH $\mu$ - $\tau$ -PHILIC HIGGS DOUBLET

The SM is extended by adding an inert Higgs doublet  $\Phi_2$  under an abelian discrete  $Z_4$  symmetry, and the  $Z_4$  charge assignment is shown in Table I [33]. The scalar potential is

TABLE I: The  $Z_4$  charge assignment.

	$Q_L^i$	$U_R^i$	$D_R^i$	$L_L^e$	$L_L^\mu$	$L_L^\tau$	$e_R$	$\mu_R$	$\tau_R$	$\Phi_1$	$\Phi_2$
$Z_4$	1	1	1	1	$i$	$-i$	1	$i$	$-i$	1	-1

given as

$$\begin{aligned}
 V = & Y_1(\Phi_1^\dagger \Phi_1) + Y_2(\Phi_2^\dagger \Phi_2) + \frac{\lambda_1}{2}(\Phi_1^\dagger \Phi_1)^2 + \frac{\lambda_2}{2}(\Phi_2^\dagger \Phi_2)^2 \\
 & + \lambda_3(\Phi_1^\dagger \Phi_1)(\Phi_2^\dagger \Phi_2) + \lambda_4(\Phi_1^\dagger \Phi_2)(\Phi_2^\dagger \Phi_1) \\
 & + \left[ \frac{\lambda_5}{2}(\Phi_1^\dagger \Phi_2)^2 + \text{h.c.} \right].
 \end{aligned} \tag{2}$$

We discuss the CP-conserving scenario in which all  $\lambda_i$  are real. The two complex scalar doublets can be given as

$$\Phi_1 = \begin{pmatrix} G^+ \\ \frac{1}{\sqrt{2}}(v + h + iG^0) \end{pmatrix}, \quad \Phi_2 = \begin{pmatrix} H^+ \\ \frac{1}{\sqrt{2}}(H + iA) \end{pmatrix}.$$

The  $\Phi_1$  field has the vacuum expectation value (VEV)  $v=246$  GeV, and the VEV of  $\Phi_2$  field is zero. The  $Y_1$  is determined by requiring the scalar potential minimization condition.

$$Y_1 = -\frac{1}{2}\lambda_1 v^2. \tag{3}$$

The Nambu-Goldstone bosons  $G^0$  and  $G^+$  are eaten by the gauge bosons. The  $H^+$  and  $A$  are the mass eigenstates of the charged Higgs boson and CP-odd Higgs boson. Their masses are given as

$$m_{H^\pm}^2 = Y_2 + \frac{\lambda_3}{2}v^2, \quad m_A^2 = m_{H^\pm}^2 + \frac{1}{2}(\lambda_4 - \lambda_5)v^2. \tag{4}$$

The  $h$  is the SM-like Higgs, and has no mixing with the inert CP-even Higgs  $H$ . Their masses are given as

$$m_h^2 = \lambda_1 v^2 \equiv (125 \text{ GeV})^2, \quad m_H^2 = m_A^2 + \lambda_5 v^2. \tag{5}$$

We obtain the masses of fermions via the Yukawa interactions with  $\Phi_1$ ,

$$-\mathcal{L} = y_u \overline{Q}_L \tilde{\Phi}_1 U_R + y_d \overline{Q}_L \Phi_1 D_R + y_\ell \overline{L}_L \Phi_1 E_R + \text{h.c.}, \tag{6}$$

where  $\tilde{\Phi}_1 = i\tau_2 \Phi_1^*$ ,  $Q_L^T = (u_{Li}, d_{Li})$ ,  $L_L^T = (\nu_{Li}, \ell_{Li})$  with  $i$  being generation indices.  $U_R$ ,  $D_R$ , and  $E_R$  are the three generation right-handed fields of the up-type quark, down-type quark,

and charged lepton. Under the  $Z_4$  symmetry, the lepton Yukawa matrix  $y_\ell$  to be diagonal. As a result, the lepton fields ( $L_L$ ,  $E_R$ ) are mass eigenstates.

Under the  $Z_4$  symmetry, the  $\Phi_2$  is allowed to have  $\mu$ - $\tau$  interactions [33],

$$-\mathcal{L}_{LFV} = \sqrt{2} \rho_{\mu\tau} \overline{L}_L^\mu \Phi_2 \tau_R + \sqrt{2} \rho_{\tau\mu} \overline{L}_L^\tau \Phi_2 \mu_R + \text{h.c.} \quad (7)$$

The interactions of Eq. (7) lead to the  $\mu$ - $\tau$  LFV couplings of  $H$ ,  $A$ , and  $H^\pm$ . We take the CP-conserving Yukawa matrix, namely that  $\rho_{\mu\tau}$  and  $\rho_{\tau\mu}$  are real and  $\rho_{\mu\tau} = \rho_{\tau\mu} \equiv \rho$ .

The SM-like Higgs  $h$  has the same tree-level couplings to fermions and gauge boson as the SM, and has no  $\mu$ - $\tau$  LFV coupling. The  $H$ ,  $A$ , and  $H^\pm$  have the  $\mu$ - $\tau$ -philic Yukawa couplings and no other Yukawa couplings. There are no cubic interactions with  $ZZ$ ,  $WW$  for the neutral Higgses  $A$  and  $H$ .

### III. MUON $g - 2$ , LUF IN $\tau$ DECAYS, LHC DATA, AND RELEVANT CONSTRAINTS

In our calculations, the input parameters are  $\lambda_2$ ,  $\lambda_3$ ,  $m_h$ ,  $m_H$ ,  $m_A$  and  $m_{H^\pm}$  which can determine the values of  $\lambda_1$ ,  $\lambda_5$  and  $\lambda_4$  from Eqs. (4, 5). We take  $m_h = 125$  GeV, and scan over several key parameters in the following ranges:

$$\begin{aligned} 0 < \rho < 1.0, \quad 5 \text{ GeV} < m_H < 115 \text{ GeV}, \\ 130 \text{ GeV} < m_A < 900 \text{ GeV}, \quad 90 \text{ GeV} < m_{H^\pm} < 900 \text{ GeV}. \end{aligned} \quad (8)$$

The  $\lambda_2$  controls the quartic couplings of extra Higgses, and does not affect the observables considered in our paper. We choose  $\lambda_3 = \lambda_4 + \lambda_5$  which leads the  $hHH$  coupling to be absent. At the tree-level, the SM-like Higgs  $h$  has the same couplings to the SM particles as the SM and no exotic decay mode. Since the extra Higgses have no couplings to quarks, we may safely neglect the bounds of meson observable **HiggsBounds** [39] is used to implement the exclusion constraints from the searches for the neutral and charged Higgs at the LEP at 95% confidence level. In addition, we consider other observables and constraints:

- (1) Theoretical constraints and the oblique parameters. We use the 2HDMC [40] to implement the theoretical constraints from the vacuum stability, unitarity and coupling-constant perturbativity, and calculate the oblique parameters ( $S$ ,  $T$ ,  $U$ ). According

to the recent fit results of Ref. [41], we take the following values of  $S$ ,  $T$ ,  $U$ ,

$$S = 0.02 \pm 0.10, \quad T = 0.07 \pm 0.12, \quad U = 0.00 \pm 0.09. \quad (9)$$

The correlation coefficients are given by

$$\rho_{ST} = 0.92, \quad \rho_{SU} = -0.66, \quad \rho_{TU} = -0.86. \quad (10)$$

The oblique parameters favor one of  $H$  and  $A$  to have a small mass splitting from  $H^\pm$ .

- (2) Muon  $g-2$ . In the model, the new contribution to muon  $g-2$  comes from the one-loop diagrams involving the  $\mu$ - $\tau$  LFV coupling of  $H$  and  $A$  [27],

$$\delta a_\mu = \frac{m_\mu m_\tau \rho^2}{8\pi^2} \left[ \frac{(\log \frac{m_H^2}{m_\tau^2} - \frac{3}{2})}{m_H^2} - \frac{\log(\frac{m_A^2}{m_\tau^2} - \frac{3}{2})}{m_A^2} \right]. \quad (11)$$

The Eq. (11) shows that the new contributions are positive for  $m_A > m_H$ . This is reason why we take  $m_A > m_H$  in our calculations.

- (3) Lepton universality in the  $\tau$  decays. The HFAG collaboration reported three ratios from pure leptonic processes, and two ratios from semi-hadronic processes,  $\tau \rightarrow \pi/K\nu$  and  $\pi/K \rightarrow \mu\nu$  [42]

$$\begin{aligned} \left(\frac{g_\tau}{g_\mu}\right) &= 1.0011 \pm 0.0015, & \left(\frac{g_\tau}{g_e}\right) &= 1.0029 \pm 0.0015, \\ \left(\frac{g_\mu}{g_e}\right) &= 1.0018 \pm 0.0014, & \left(\frac{g_\tau}{g_\mu}\right)_\pi &= 0.9963 \pm 0.0027, \\ \left(\frac{g_\tau}{g_\mu}\right)_K &= 0.9858 \pm 0.0071, \end{aligned} \quad (12)$$

with the definitions

$$\begin{aligned} \left(\frac{g_\tau}{g_\mu}\right)^2 &\equiv \bar{\Gamma}(\tau \rightarrow e\nu\bar{\nu})/\bar{\Gamma}(\mu \rightarrow e\nu\bar{\nu}), \\ \left(\frac{g_\tau}{g_e}\right)^2 &\equiv \bar{\Gamma}(\tau \rightarrow \mu\nu\bar{\nu})/\bar{\Gamma}(\mu \rightarrow e\nu\bar{\nu}), \\ \left(\frac{g_\mu}{g_e}\right)^2 &\equiv \bar{\Gamma}(\tau \rightarrow \mu\nu\bar{\nu})/\bar{\Gamma}(\tau \rightarrow e\nu\bar{\nu}). \end{aligned} \quad (13)$$

The correlation matrix for the above five observables is

$$\begin{pmatrix} 1 & +0.53 & -0.49 & +0.24 & +0.12 \\ +0.53 & 1 & +0.48 & +0.26 & +0.10 \\ -0.49 & +0.48 & 1 & +0.02 & -0.02 \\ +0.24 & +0.26 & +0.02 & 1 & +0.05 \\ +0.12 & +0.10 & -0.02 & +0.05 & 1 \end{pmatrix}. \quad (14)$$

The  $\bar{\Gamma}$  denotes the partial width normalized to its SM value. In this model, we have

$$\begin{aligned} \bar{\Gamma}(\tau \rightarrow \mu\nu\bar{\nu}) &= (1 + \delta_{\text{loop}}^\tau)^2 (1 + \delta_{\text{loop}}^\mu)^2 + \delta_{\text{tree}}, \\ \bar{\Gamma}(\tau \rightarrow e\nu\bar{\nu}) &= (1 + \delta_{\text{loop}}^\tau)^2, \\ \bar{\Gamma}(\mu \rightarrow e\nu\bar{\nu}) &= (1 + \delta_{\text{loop}}^\mu)^2. \end{aligned} \quad (15)$$

Where  $\delta_{\text{tree}}$  can give a positive correction to  $\tau \rightarrow \mu\nu\bar{\nu}$ , and is from the tree-level diagram mediated by the charged Higgs,

$$\delta_{\text{tree}} = 4 \frac{m_W^4 \rho^4}{g^4 m_{H^\pm}^4}. \quad (16)$$

$\delta_{\text{loop}}^\tau$  and  $\delta_{\text{loop}}^\mu$  are the corrections to vertices  $W\bar{\nu}_\tau\tau$  and  $W\bar{\nu}_\mu\mu$ , which are from the one-loop diagrams involving  $H$ ,  $A$ , and  $H^\pm$ . Since we take  $\rho_{\mu\tau} = \rho_{\tau\mu}$  in the lepton Yukawa matrix, and therefore  $\delta_{\text{loop}}^\tau = \delta_{\text{loop}}^\mu$ . Following the results of [12, 14, 33],

$$\delta_{\text{loop}}^\tau = \delta_{\text{loop}}^\mu = \frac{1}{16\pi^2} \rho^2 \left[ 1 + \frac{1}{4} (H(x_A) + H(x_H)) \right], \quad (17)$$

where  $H(x_\phi) \equiv \ln(x_\phi)(1 + x_\phi)/(1 - x_\phi)$  with  $x_\phi = m_\phi^2/m_{H^\pm}^2$ .

In the model,

$$\left( \frac{g_\tau}{g_\mu} \right)_\pi = \left( \frac{g_\tau}{g_\mu} \right)_K = \left( \frac{g_\tau}{g_\mu} \right). \quad (18)$$

We perform  $\chi_\tau^2$  calculation for the five observables. The covariance matrix constructed from the data of Eq. (12) and Eq. (14) has a vanishing eigenvalue, and the corresponding degree is removed in our calculation. In our discussions we require the value of  $\chi_\tau^2$  to be smaller than the SM value, 12.3.

- (4) Lepton universality in the  $Z$  decays. The experimental values of the ratios of the leptonic  $Z$  decay branching fractions are given as [43]:

$$\frac{\Gamma_{Z \rightarrow \tau^+ \tau^-}}{\Gamma_{Z \rightarrow e^+ e^-}} = 1.0019 \pm 0.0032, \quad (19)$$

$$\frac{\Gamma_{Z \rightarrow \mu^+ \mu^-}}{\Gamma_{Z \rightarrow e^+ e^-}} = 1.0009 \pm 0.0028, \quad (20)$$

with a correlation of +0.63. In the model, the new contributions to the widths of  $Z \rightarrow \tau^+\tau^-$  and  $Z \rightarrow \mu^+\mu^-$  are from the one-loop diagrams involving the extra Higgs bosons. The ratio of Eq. (19) is given as [12, 14, 33]

$$\frac{\Gamma_{Z \rightarrow \tau^+\tau^-}}{\Gamma_{Z \rightarrow e^+e^-}} \approx 1.0 + \frac{2g_L^e \text{Re}(\delta g_L^{\text{loop}}) + 2g_R^e \text{Re}(\delta g_R^{\text{loop}})}{g_L^e{}^2 + g_R^e{}^2}. \quad (21)$$

with the SM value  $g_L^e = -0.27$  and  $g_R^e = 0.23$ . The one-loop corrections  $\delta g_L^{\text{loop}}$  and  $\delta g_R^{\text{loop}}$  are from

$$\delta g_L^{\text{loop}} = \frac{1}{16\pi^2} \rho^2 \left\{ -\frac{1}{2} B_Z(r_A) - \frac{1}{2} B_Z(r_H) - 2C_Z(r_A, r_H) + s_W^2 \left[ B_Z(r_A) + B_Z(r_H) + \tilde{C}_Z(r_A) + \tilde{C}_Z(r_H) \right] \right\}, \quad (22)$$

$$\delta g_R^{\text{loop}} = \frac{1}{16\pi^2} \rho^2 \left\{ 2C_Z(r_A, r_H) - 2C_Z(r_{H^\pm}, r_{H^\pm}) + \tilde{C}_Z(r_{H^\pm}) - \frac{1}{2} \tilde{C}_Z(r_A) - \frac{1}{2} \tilde{C}_Z(r_H) + s_W^2 [B_Z(r_A) + B_Z(r_H) + 2B_Z(r_{H^\pm}) + \tilde{C}_Z(r_A) + \tilde{C}_Z(r_H) + 4C_Z(r_{H^\pm}, r_{H^\pm})] \right\}, \quad (23)$$

where  $r_\phi = m_\phi^2/m_Z^2$  with  $\phi = A, H, H^\pm$ , and

$$B_Z(r) = -\frac{\Delta_\epsilon}{2} - \frac{1}{4} + \frac{1}{2} \log(r), \quad (24)$$

$$C_Z(r_1, r_2) = \frac{\Delta_\epsilon}{4} - \frac{1}{2} \int_0^1 dx \int_0^x dy \log[r_2(1-x) + (r_1-1)y + xy], \quad (25)$$

$$\begin{aligned} \tilde{C}_Z(r) &= \frac{\Delta_\epsilon}{2} + \frac{1}{2} - r[1 + \log(r)] + r^2[\log(r) \log(1+r^{-1}) \\ &\quad - \text{Li}_2(-r^{-1})] - \frac{i\pi}{2} [1 - 2r + 2r^2 \log(1+r^{-1})]. \end{aligned} \quad (26)$$

Besides,  $\Gamma_{Z \rightarrow \mu^+\mu^-}$  equals to  $\Gamma_{Z \rightarrow \tau^+\tau^-}$  for  $\rho_{\mu\tau} = \rho_{\tau\mu}$ .

(5) The multi-lepton searches at the LHC. The  $H$ ,  $A$ , and  $H^\pm$  are mainly produced at the LHC via the electroweak processes:

$$pp \rightarrow W^{\pm*} \rightarrow H^\pm A, \quad (27)$$

$$pp \rightarrow Z^* \rightarrow H A, \quad (28)$$

$$pp \rightarrow W^{\pm*} \rightarrow H^\pm H, \quad (29)$$

$$pp \rightarrow Z^*/\gamma^* \rightarrow H^+ H^-. \quad (30)$$

$$pp \rightarrow Z \rightarrow \tau^\pm \mu^\mp H. \quad (31)$$

When  $H$ ,  $A$ , and  $H^\pm$  have small splitting mass, the main decay modes of these Higgses are

$$H \rightarrow \tau^\pm \mu^\mp, \quad A \rightarrow \tau^\pm \mu^\mp, \quad H^\pm \rightarrow \tau^\pm \nu_\mu, \mu^\pm \nu_\tau. \quad (32)$$

For  $m_A$  ( $m_{H^\pm}$ )  $> m_H + m_Z$ , the following exotic decay modes will open,

$$A \rightarrow HZ, \quad H^\pm \rightarrow HW^\pm. \quad (33)$$

We perform simulations for the processes employing `MG5_aMC-2.4.3` [44] with `PYTHIA6` [45] and `Delphes-3.2.0` [46], and impose the constraints from all the analysis at the 13 TeV LHC in the latest `CheckMATE 2.0.28` [47] and `Fastjet` [48]. The analysis we implemented in our previous works [35, 49] are also included. Besides, we impose the recently published analyses of searching for events with three or more leptons, with up to two hadronical  $\tau$  leptons, using 13 TeV LHC 137 fb $^{-1}$  data [50]. It improves significantly the limits on new physical particles that decay to leptons. The signal regions of 41I, 41J and 41K, which require 4 leptons with one or two hadronical  $\tau$  leptons in the final states, are most sensitive to our samples, because of the dominated multi-lepton final states in our model.

#### IV. RESULTS AND DISCUSSIONS

We impose the constraints of "pre-muon  $g - 2$ " (denoting the theory, the oblique parameters, the exclusion limits from the searches for Higgs at LEP), and show the surviving samples with  $\chi_\tau^2 < 12.3$  fitting the data of LUF in  $\tau$  decays in Fig. 1. For a very small  $\rho$ , the new contributions to  $\tau$  decays disappear, and therefore the value of  $\chi_\tau^2$  approaches to the SM value, 12.3. The discrepancy of LUF in  $\tau$  decays can be alleviated by enhancing  $\Gamma(\tau \rightarrow \mu\nu\bar{\nu})$ . From Eq. (15), we can find that  $\tau \rightarrow \mu\nu\bar{\nu}$  receives the corrections from the one-loop diagram and tree-level diagram mediated by the charged Higgs. According to Eq. (17), the former tends to give the negative corrections and enhance the value of  $\chi_\tau^2$ . According to Eq. (16), the latter gives the positive corrections and reduce the value of  $\chi_\tau^2$ . In order to obtain  $\chi_\tau^2 < 12.3$  for a large  $m_{H^\pm}$ , a large  $\rho$  is required to make the contributions of tree-level diagram to overcome those of one-loop diagram since the contributions of tree-level diagram are suppressed by  $m_{H^\pm}$ . For  $\chi_\tau^2 < 9.7$ ,  $\rho$  is always required to increase with  $m_{H^\pm}$  and be larger than 0.11.



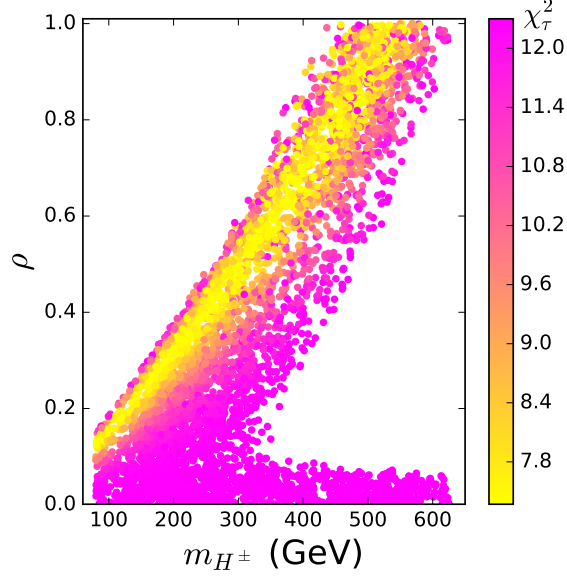


FIG. 1: The surviving samples satisfying the constraints of "pre-muon  $g - 2$ " and  $\chi_\tau^2 < 12.3$  projected on the plane of  $\rho$  versus  $m_{H^\pm}$ .

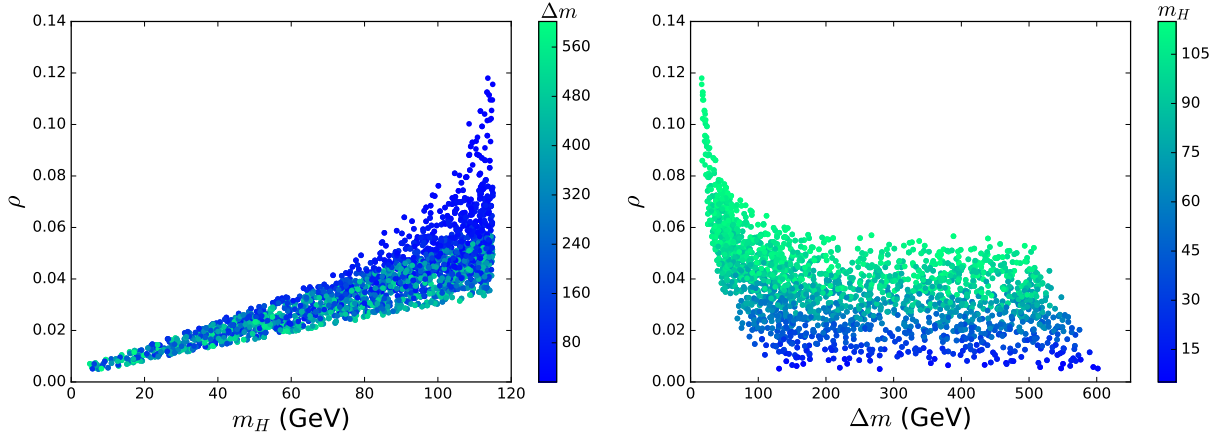


FIG. 2: The surviving samples satisfying the constraints of "pre-muon  $g - 2$ " and muon  $g - 2$  anomaly projected on the planes of  $\rho$  versus  $m_H$  and  $\rho$  versus  $\Delta m$ .

After imposing the constraints of "pre-muon  $g - 2$ " and muon  $g - 2$ , we project the surviving samples on the planes of  $\rho$  versus  $m_H$  and  $\rho$  versus  $\Delta m$  ( $\Delta m = m_A - m_H$ ) in Fig. 2. From the Eq. (11), we can find that  $\Delta a_\mu$  receives a positive correction from the diagrams involving  $H$  and a negative correction from ones involving  $A$ . As a result,  $\Delta a_\mu$  is sizable enhanced by a large mass splitting between  $m_A$  and  $m_H$  ( $\Delta m$ ), and favors  $\rho$  to decrease with an increase of  $\Delta m$ , as shown in the right panel of Fig. 2. In addition, the Eq. (11) shows that the contributions of the diagrams involving  $H$  and  $A$  to  $\Delta a_\mu$  are respectively

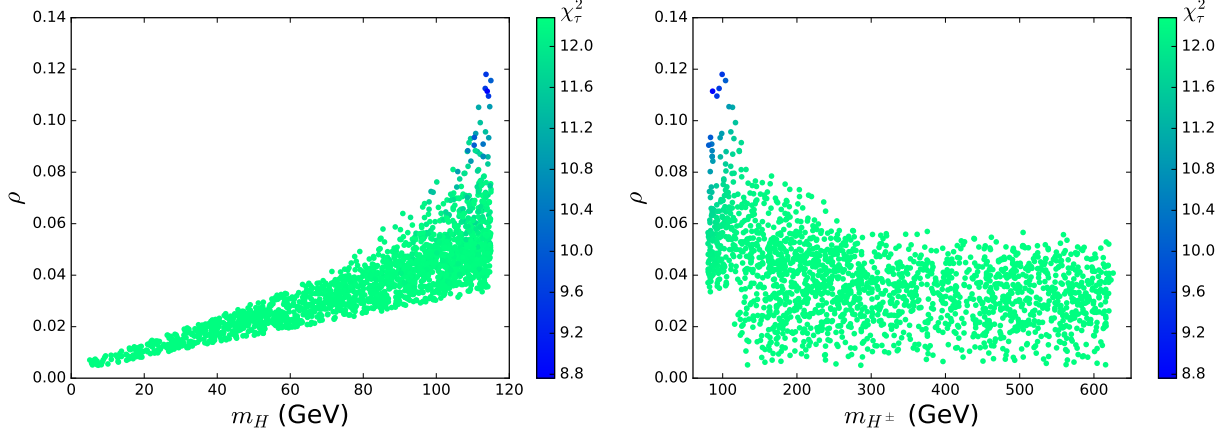


FIG. 3: The surviving samples satisfying the constraints of "pre-muon  $g-2$ ", muon  $g-2$  anomaly,  $\chi_\tau^2 < 12.3$ , and  $Z$  decays.

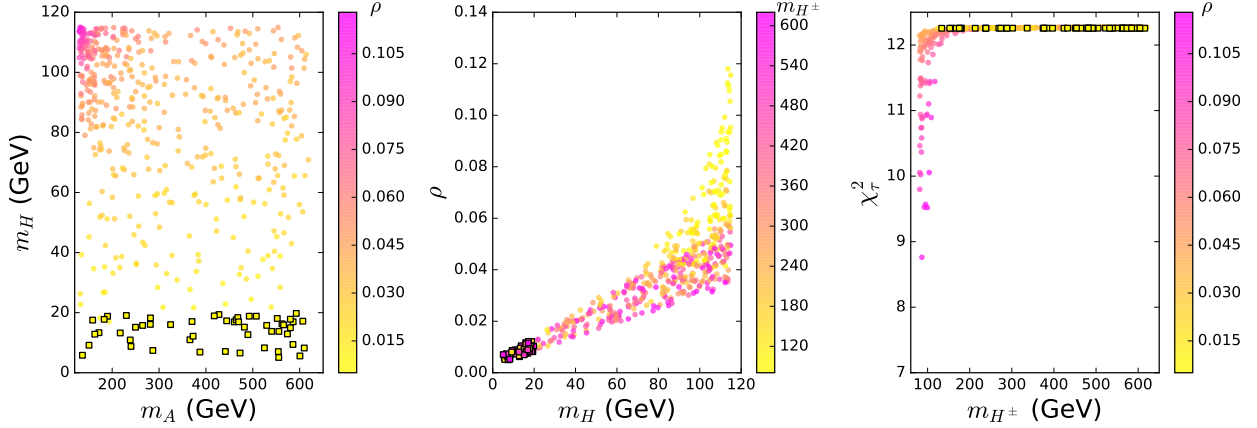


FIG. 4: The surviving samples on the planes of  $m_H$  versus  $m_A$ ,  $\rho$  versus  $m_H$ , and  $\chi_\tau^2$  versus  $m_{H^\pm}$ . All the samples satisfy the constraints of "pre-muon  $g-2$ ", muon  $g-2$  anomaly,  $\chi_\tau^2 < 12.3$ , and  $Z$  decays. The bullets and squares are excluded and allowed by the direct searches at the LHC.

suppressed by  $m_H^2$  and  $m_A^2$ . Therefore,  $\Delta a_\mu$  favors  $\rho$  to increase with  $m_H$ , as shown in the left panel of Fig. 2. The muon  $g-2$  anomaly can be explained in the parameter space of  $0.005 < \rho < 0.12$  and  $5 \text{ GeV} < m_H < 115 \text{ GeV}$ .

In Fig. 3, we show the surviving samples after imposing the constraints of "pre-muon  $g-2$ ", muon  $g-2$ ,  $\chi_\tau^2 < 12.3$ , and  $Z$  decays. Since the muon  $g-2$  anomaly favors  $0.005 < \rho < 0.12$ , most of the parameter space satisfying  $\chi_\tau^2 < 12.3$  are excluded. From Fig. 3, we find that a small  $\chi_\tau^2$  favors a large  $m_H$  and a small  $m_{H^\pm}$ . Since the muon  $g-2$  anomaly favors a large  $\rho$  for a large  $m_H$ , and such large  $\rho$  can enhance the width of  $\tau \rightarrow \mu\nu\nu$

and reduce the value of  $\chi_\tau^2$ .

After imposing the constraints of the direct searches at the LHC, the surviving samples of Fig. 3 are projected on Fig. 4. We find that the direct searches at the LHC impose a stringent upper bound on  $m_H$ ,  $m_H < 20$  GeV, and allow  $130 \text{ GeV} < m_A \text{ } (m_{H^\pm}) < 610 \text{ GeV}$ . For a light  $H$ , the  $\tau\mu$  from  $H$  decays become too soft to be distinguished at detector, while the  $\tau\mu$  from  $H$  in  $A/H^\pm$  decays are collinear because of the large mass splitting between  $H$  and  $A/H^\pm$ . In addition, the  $A/H^\pm \rightarrow HZ/W^\pm$  decay modes dominate the  $A/H^\pm$  decays in the low  $m_H$  region. Thus, in the region of  $m_H < 20$  GeV, the acceptance of above signal region for final state of collinear  $\tau\mu + Z/W$  boson quickly decreases. For  $5 \text{ GeV} < m_H < 20$  GeV, the muon  $g - 2$  anomaly favors  $0.005 < \rho < 0.014$ . As a result, the new contributions to the  $\tau$  decays are very small, and the  $\chi_\tau^2$  approaches to the value of SM, 12.3.

## V. CONCLUSION

In the 2HDM with an abelian discrete  $Z_4$  symmetry, one Higgs doublet has the same interactions with fermions as the SM, and another inert Higgs doublet only has the  $\mu$ - $\tau$  LFV interactions. After imposing various relevant theoretical and experimental constraints, especially for the multi-lepton search at the LHC, we found that the model can explain the muon  $g - 2$  anomaly within  $2\sigma$  range in the region of  $5 \text{ GeV} < m_H < 20 \text{ GeV}$ ,  $130 \text{ GeV} < m_A \text{ } (m_{H^\pm}) < 610 \text{ GeV}$ , and  $0.005 < \rho < 0.014$ . Meanwhile, the  $\chi_\tau^2$  fitting the data of LFU in the  $\tau$  decays approaches to the SM prediction.

## Acknowledgment

This work was by the National Natural Science Foundation of China under grant 11975013, by the Natural Science Foundation of Shandong province (ZR2017JL002 and ZR2017MA004), and by the Project of Shandong Province Higher Educational Science and Technology Program under Grants No. 2019KJJ007.

- 
- [1] Muon  $g-2$  Collaboration], Phys. Rev. Lett. **86**, (2001) 2227; Phys. Rev. D **73**, (2006) 072003.
  - [2] B. Abi *et al.* [Fermilab Collaboration], Phys. Rev. Lett. **126**, (2021) 141801.

- [3] A. Dedes and H. E. Haber, JHEP **0105**, (2001) 006.
- [4] D. Chang, W.-F. Chang, C.-H. Chou, and W.-Y. Keung, Phys. Rev. D **63**, (2001) 091301.
- [5] K. M. Cheung, C. H. Chou and O. C. W. Kong, Phys. Rev. D **64**, (2001) 111301.
- [6] J. Cao, P. Wan, L. Wu and J. M. Yang, Phys. Rev. D **80**, (2009) 071701.
- [7] L. Wang and X. F. Han, JHEP **05**, (2015) 039.
- [8] E. J. Chun, Z. Kang, M. Takeuchi, Y.-L. Tsai, JHEP **1511**, (2015) 099.
- [9] A. Cherchiglia, P. Kneschke, D. Stockinger, H. Stockinger-Kim, JHEP **1701**, (2017) 007.
- [10] X. Liu, L. Bian, X.-Q. Li, J. Shu, Nucl. Phys. B **909**, (2016) 507-524.
- [11] X.-F. Han, T. Li, L. Wang, Y. Zhang, Phys. Rev. D **99**, (2019) 095034.
- [12] T. Abe, R. Sato and K. Yagyu, JHEP **1507**, (2015) 064.
- [13] A. Crivellin, J. Heeck, P. Stoffer, Phys. Rev. Lett. **116**, (2016) 081801.
- [14] E. J. Chun, J. Kim, JHEP **1607**, (2016) 110.
- [15] L. Wang, J. M. Yang, M. Zhang, Y. Zhang, Phys. Lett. B **788**, (2019) 519-529.
- [16] T. Han, S. K. Kang, J. Sayre, JHEP **1602**, (2016) 097.
- [17] V. Ilisie, JHEP **1504**, (2015) 077.
- [18] O. Eberhardt, A. Martínez, A. Pich, arXiv:2012.09200.
- [19] S.-P. Li, X.-Q. Li, Y. Li, Y.-D. Yang, X. Zhang, JHEP **2101**, (2021) 034.
- [20] S.-P. Li, X.-Q. Li, Y.-D. Yang, Phys. Rev. D **99**, (2019) 035010.
- [21] N. Ghosh, J. Lahiri, arXiv:2103.10632.
- [22] S. Jana, P. K. Vishnu, S. Saad, Phys. Rev. D **101**, (2020) 115037.
- [23] N. Chen, B. Wang, C. Yao, arXiv:2102.05619.
- [24] F. J. Botella, F. Cornet-Gomez, M. Nebot, Phys. Rev. D **102**, 035023 (2020).
- [25] E. J. Chun, T. Mondal, Phys. Lett. B **802**, (2020) 135190.
- [26] K. Adikle Assamagan, A. Deandrea, P.-A. Delsart, Phys. Rev. D **67**, (2003) 035001.
- [27] S. Davidson, G. J. Grenier, Phys. Rev. D **81**, (2010) 095016.
- [28] Y. Omura, E. Senaha, K. Tobe, JHEP **1505**, (2015) 028.
- [29] R. Benbrik, C.-H. Chen, T. Nomura, Phys. Rev. D **93**, (2016) 095004.
- [30] Y. Omura, E. Senaha, K. Tobe, Phys. Rev. D **94**, (2016) 055019.
- [31] M. Lindner, M. Platscher, F. S. Queiroz, Phys. Rept. **731**, (2018) 1-82.
- [32] L. Wang, S. Yang, X.-F. Han, Nucl. Phys. B **919**, (2017) 123-141.
- [33] Y. Abe, T. Toma, K. Tsumura, JHEP **1906**, (2019) 142.

- [34] S. Iguro, Y. Omura, M. Takeuchi, JHEP **1911**, (2019) 130.
- [35] L. Wang, Y. Zhang, Phys. Rev. D **100**, (2019) 095005.
- [36] S. Iguro, Y. Omura, M. Takeuchi, JHEP **09**, (2020) 144.
- [37] A. Crivellin, D. Müller, C. Wiegand, JHEP **06**, (2019) 119.
- [38] A. Das, T.i Nomura, H. Okada, S. Roy, Phys. Rev. D **96**, (2017) 075001.
- [39] P. Bechtle, O. Brein, S. Heinemeyer, G. Weiglein, K. E. Williams, Comput. Phys. Commun. **181**, (2010) 138-167.
- [40] D. Eriksson, J. Rathsmann, O. Stål, Comput. Phys. Commun. **181**, (2010) 189.
- [41] M. Tanabashi et al., [Particle Data Group], Phys. Rev. D **98**, 030001 (2018).
- [42] Y. Amhis et al. [Heavy Flavor Averaging Group (HFAG) Collaboration], arXiv:1412.7515.
- [43] S. Schael et al. [ALEPH and DELPHI and L3 and OPAL and SLD and LEP Electroweak Working Group and SLD Electroweak Group and SLD Heavy Flavour Group Collaborations], Phys. Rept. **427**, (2006) 257.
- [44] J. Alwall *et al.*, JHEP **1407**, (2014) 079.
- [45] P. Torrielli and S. Frixione, JHEP **1004**, (2010) 110.
- [46] J. de Favereau *et al.* [DELPHES 3 Collaboration], JHEP **1402**, (2014) 057.
- [47] D. Dercks, N. Desai, J. S. Kim, K. Rolbiecki, J. Tattersall and T. Weber, Comput. Phys. Commun. **221**, (2017) 383.
- [48] M. Cacciari, G. P. Salam and G. Soyez, Eur. Phys. J. C **72** (2012), 1896.
- [49] G. Pozzo and Y. Zhang, Phys. Lett. B **789**, (2019) 582-591.
- [50] A. M. Sirunyan *et al.* [CMS Collaboration], CMS-PAS-SUS-19-012.